Heliyon 10 (2024) e32794

Contents lists available at ScienceDirect

Heliyon

journal homepage: www.cell.com/heliyon

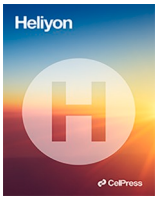

Research article

Thermal, viscoelastic, and electrical properties of thermoplastic polyurethane films reinforced with multi-walled carbon nanotubes

Jose Munoz Chilito [a], Jose A. Lara-Ramos [a], JulianA. Angel [b], Fiderman Machuca-Martínez [c,d], Lorena Marín [c,e], Luis A. Rodríguez [a,c], Juan P. Correa Aguirre [f], Miguel A. Hidalgo Salazar [f], Serafin García-Navarro [g], Luis Roca-Blay [g], Jesús E. Diosa [a,c,**], Edgar Mosquera-Vargas [a,c,*]

[a] *Grupo de Transiciones de Fase y Materiales Funcionales (GTFMF), Departamento de Física, Universidad del Valle, A.A, 25360, Cali, Colombia*
[b] *Departamento de Ciencias Básicas, Institución Universitaria Antonio José Camacho, Avenida 6N No 28N-102, A.A, 25663, Cali, Colombia*
[c] *Centro de Excelencia en Nuevos Materiales (CENM), Universidad del Valle, A.A, 25663, Cali, Colombia*
[d] *Grupo de Investigación en Procesos Avanzados para Tratamientos biológicos y Químicos (GAOX), Escuela de Ingeniería Química, Universidad del Valle, A.A, 25663, Cali, Colombia*
[e] *Grupo de Películas Delgadas (GPD), Universidad del Valle, A.A, 25663, Cali, Colombia*
[f] *Grupo de Investigación en Tecnología para la Manufactura (GITEM), Universidad Autónoma de Occidente, 760035, Cali, Colombia*
[g] *AIMPLAS, Gustave Eiffel 4 (València Parc Tecnològic), 46980, Paterna, Spain*

ARTICLE INFO

Keywords:
Nanomaterial-reinforced polymer films
Viscoelastic properties
Electrical properties

ABSTRACT

Thermoplastic polyurethane (TPU) doped with multi-walled carbon nanotubes (MWCNTs) at 1, 3, 5, and 7 wt% has been studied. The effect of MWCNTs on thermal, viscoelastic, and electric properties in the TPU matrix was characterized by differential scanning calorimetry (DSC), dynamic mechanical analysis (DMA), and by impedance spectroscopy. The results show that the thermal, electrical, and viscoelastic properties, such as the glass transition temperature, shifted towards high temperatures. The melting temperature decreased, and the conductivity and the storage modulus increased by 61.5 % and 58.3 %. The previously observed behavior on the films is due to the increase in the mass percentage of carbon nanotubes (CNTs) in the TPU matrix. Also, it can be said that the CNTs were homogeneously dispersed in the TPU matrix, preventing the movement of the polymer chains, and generating channels or connections that increase the conductivity and improve the thermal properties of the material.

1. Introduction

Nanoreinforced materials have emerged as an alternative to solve various problems within the science of composite materials. It is

* Corresponding author.
** Corresponding author.
E-mail addresses: jose.chilito@correounivalle.edu.co (J.M. Chilito), lara.jose@correounivalle.edu.co (J.A. Lara-Ramos), aangel@admon.uniajc.edu.co (JulianA. Angel), fiderman.machuca@correounivalle.edu.co (F. Machuca-Martínez), marin.lorena@correounivalle.edu.co (L. Marín), luis.a.rodriguez@correounivalle.edu.co (L.A. Rodríguez), jpcorrea@uao.edu.co (J.P. Correa Aguirre), mahidalgo@uao.edu.co (M.A. Hidalgo Salazar), sgarcia@aimplas.es (S. García-Navarro), lroca@aimplas.es (L. Roca-Blay), jesus.diosa@correounivalle.edu.co (J.E. Diosa), edgar.mosquera@correounivalle.edu.co (E. Mosquera-Vargas).

https://doi.org/10.1016/j.heliyon.2024.e32794
Received 22 August 2023; Received in revised form 22 March 2024; Accepted 10 June 2024
Available online 11 June 2024

Table 1
Geometric parameters: thickness, width, and length for TPU films with 1, 3, 5, 7 % wt MWCNTs.

Parameters	TPU/MWCNTs sample			
	1 % wt	3 % wt	5 % wt	7 % wt
Length (mm)	40.23 ± 0.10	40.14 ± 0.10	39.53 ± 0.10	40.31 ± 0.10
Width (mm)	5.98 ± 0.10	5.88 ± 0.04	5.63 ± 0.10	5.78 ± 0.10
Thickness (mm)	1.61 ± 0.01	1.74 ± 0.02	1.79 ± 0.01	1.87 ± 0.01

common to use synthetic and natural fibers in combination with polymeric matrices, aiming to improve some properties by nano-reinforcing the fibers to the polymer [1–3]. Now, a compatible mixture based on elastomers such as TPU is common for developing new materials in different applications such as energy storage, automotive components, environmental solutions, medical devices, among others [4]. Some examples are Wung et al. [5] who studied the effect of PVC on the morphology of the mixture with segmented TPU. Here, PVC was shown to be miscible in the TPU matrix [4]. But previously, Laukaitienė et al. [6] reported that increasing the TPU matrix's PVC content increases the degree of dissolution of the soft and rigid segments in the TPU matrix. On the other hand, Jeong et al. [7] found that the increase in PVC volume decreases the hysteresis in the repeated cyclic test.

Therefore, research is being carried out on the use of nanofillers such as carbon nanotubes, nanoclays, graphene nanostructures, nanofillers, among others, to improve the properties of miscible mixtures [4,8,9]. These nanostructures improve the mechanical properties and stiffness of new composite materials but also serve as fixed structures that improve the material electrical and shape memory behaviours [10]. However, the current challenges are to obtain polymeric matrices with an adequate dispersion of nano-particles that allow overcoming limitations during applications that require super thin homogeneous properties on the surface or volume of the material. One of the nano-reinforcements with many publications are multi-walled carbon nanotubes (MWCNTs) which, due to their characteristics (such as low density, excellent mechanical strength, thermal stability, and high thermal and electrical conductivity), allow the improvement of morphological, structural, and electrical properties of polymer-based composite materials such as TPU. However, the potential use of carbon nanotubes as reinforcing agents in polymer nanocomposites can only be achieved when their optimal dispersion in the matrix is ensured [11]. But this optimal dispersion is not easy to achieve in viscous polymeric matrices due to the intrinsic nature of CNTs, where there are always interlocked or agglomerated carbon structures due to the van de Waals intermolecular interactions. Therefore, previous works have reported that chemical modifications to carbon nanotubes are required to improve dispersion and adhesion within the polymer matrix [11].

Based on the above considerations, the objective of this research is to investigate the influence and reinforcement of the content of carbon nanotubes (at 1 %, 3 %, 5 % and 7 % by weight) in the polymeric structure of thermoplastic polyurethane (TPU) films provided by the Technological Institute of Plastics - AIMPLAST of Spain. The purpose is to study the thermal, mechanical, and electrical properties of the resulting films.

2. Materials and methods

2.1. Materials

For the construction of the TPU Films, it was used as received for this study. Carbon nanotubes were purchased from NANOCYL®, Belgium. The MWCNTs have a mean length of 1.5 μm, a mean diameter of 9.5 nm, and a carbon purity of 90 %. The electrical and mechanical characterization of the nanocomposite material is presented in our previous work reported in Ref. [12].

2.2. Preparation of TPU/MWCNTs nanocomposite films

TPU Pellets and TPU/MWCNTs nanocomposite Pellets with 1, 3, 5, 7 at wt% of MWCNTs were processed by compression molding in a hot plate press LabPro400 Fontijne Press (Netherlands) with stainless steel frames with 200 μm. The process parameters used were 10 kN compression force for 5 min at 200 °C.

2.3. Characterizations

Several analytical, mechanical, and electrical methods are described to characterize the films composed of TPU/MWCNTs.

2.3.1. DSC studies

Differential Scanning Calorimeter (DSC), model TA Instruments Q100 was used to measure the enthalpies and temperatures of the various thermal events of the different TPU/MWCNTs nanocomposite plate samples when they are thermally treated. Each sample was first subjected to a thermal cycle from 20 to 180 °C; then two cycles of heating and cooling from 180 to −80 °C (the last heating cycle was up to 300 °C) at a rate of 8 °C/min to remove the absorbed water. All heating and cooling runs were evaluated under 50 ml/min nitrogen gas flow.

2.3.2. Dynamic mechanical analysis

The viscoelastic behavior of the TPU/MWCNTs films was carried out in a DMA RSA-G2 (Texas Instruments, Dallas, TX, USA)

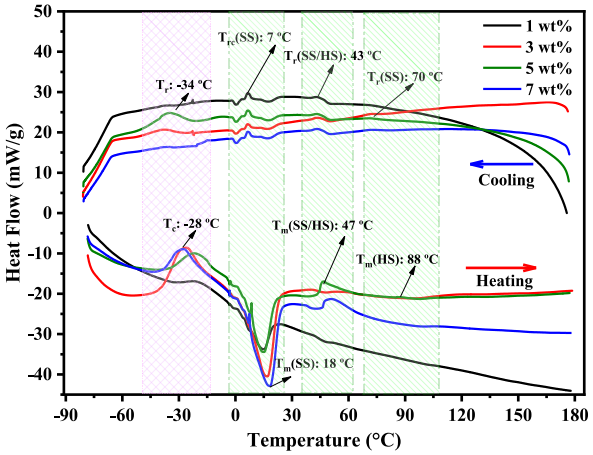

Fig. 1. DSC thermograms of TPU/(1, 3, 5, 7 % wt) MWCNTs.

equipped with an air chiller unit ACS-3. To identify the studied materials, the following test modes were performed.

2.3.2.1. Strain sweep tests. To identify the linear viscoelastic region, strain sweeps were performed using a tension geometry. The tests were performed at temperatures of −50 and 80 °C, with a frequency of 1 Hz and a range of strains from 0.001 % to 1 %. Table 1 shows the width, length, and thickness values used in the samples analyzed in the tests for the loss and storage modulus as a function of temperature for samples 1, 3, 5, 7 % wt. MWCNTs.

2.3.2.2. Temperature ramp tests. The temperature ramp tests were performed between −80 °C and 150 °C, at 1 Hz, 5 °C/min, and 0.15 % strain (taken from the linear viscoelastic domain of the plot E′ vs. strain obtained in the strain sweep tests). The effect of carbon nanotubes loading in storage modulus (E′), and Tan(delta) (loss factor) values were recorded.

2.3.3. Impedance spectroscopy studies

The electrical properties of the films were characterized using a Wayne Kerr 6420 impedance analyzer with an excitation signal of 100 mV, which measured impedance data in the frequency range of 20Hz to 500 kHz. The films were measured using a two-electrode configuration, with gold as electrodes. To estimate the relevant electrical parameters of the films, an equivalent circuit model inspired by Ref. [12] was employed. This model provides the resistance (R) associated with each conduction mechanism. By employing the equation $\sigma = d/AR$ (d and A represent the thickness and area of the films, respectively), the conductivities of each conduction mechanism were calculated.

3. Results and discussion

3.1. The thermal properties

3.1.1. Glass transition temperature, melting temperature, hard segments, and soft segments

Fig. 1 shows the DSC scan for samples with 1, 3, 5, and 7 % by weight of MWCNTs during both heating (a trend with a red arrow) and cooling (a trend with a blue arrow) processes. In the heating scan, the curve exhibits the typical melting temperature associated with the TPU matrix [3,13,14]. In the region close to −28 °C, a broad exothermic peak is observed, which can be attributed to the crystallization temperature (T_c) of the soft segments of the TPU [3,15,16]; in samples containing 1 %, 3 %, 5 %, and 7 % wt. MWCNTs. Meanwhile, T_g is not displayed clearly on the thermogram.

In addition to the low-temperatures, all samples exhibited three endothermic transitions. The first transition (T_m(SS)) occurred between approximately −3 °C and 26 °C and is associated with the melting temperature of soft segments (SS). The second transition (T_m(SS/HS)) occurred around 47 °C and is linked to the interactions between the soft and hard segments (HS). Particularly, the disorder of hard segments not ideally packed in the interfacial region between the soft and hard phases [17]. The third transition (T_m(HS)) took place at approximately 80 °C and corresponds to the melting temperatures associated with the short-range and long-range ordering of the hard segments [18,19].

Lastly, in the cooling scan for temperature values above −1 °C, three exothermic bands are observed; each of these bands is associated with a recrystallization temperature (T_r) which is strongly linked with the endothermic bands studied previously [20]. In addition, the exothermic band found around −34 °C could be related to the recrystallization of the soft segments [21,22].

3.1.2. Enthalpies and characteristic peaks for DCS sweeps

Fig. 2 shows the enthalpies associated with the bands observed in the DCS of TPU films with different concentrations of carbon

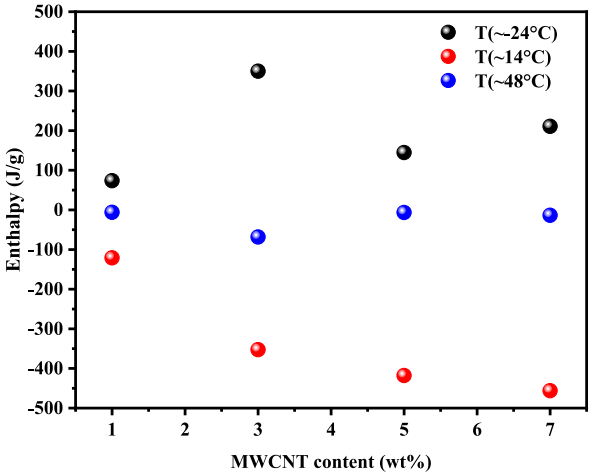

Fig. 2. Enthalpy as a Function of Multi-Walled Carbon Nanotubes concentration in TPU Films.

Table 2
Temperature data, T_{Onset} (for calculated areas), calculated enthalpy. The above information is for heating and cooling in DSC experiments for TPU/MWCNTs film samples.

TPU/MWCNTs films	−80 °C–180 °C (Heating)			180 °C to −80 °C (Cooling)		
	T_{peak} (°C)	T_{Onset} (°C)	Enthalpy (J/g)	T_{peak} (°C)	T_{Onset} (°C)	Enthalpy (J/g)
1 % wt	−22.40	−33.41	10.76↑	−36.81	−41.50	1.34↑
	2.70	0.72	1.36↓	2.480	0.60	4.58↓
	15.40	8.71	51.31↓	6.63	8.70	5.83↑
	48.10	44.33	3.50↓	23.00	18.70	6.77↓
	–	–	5.10↓	45.90	43.41	1.63↑
3 % wt	−26.70	−39.22	295.00↑	−30.43	−39.40	24.89↑
	−1.14	−4.80	0.17↓	2.50	0.47	3.85↓
	17.32	5.80	305.30↓	8.50	6.42	3.86↑
	47.50	45.32	4.80↓	23.50	19.20	5.68↓
	–	–	–	49.00	43.70	7.59↑
5 % wt	−21.00	−34.60	115.31↑	−38.84	−33.30	1.95↑
	−1.35	1.53	0.23↓	2.47	0.79	4.51↓
	15.53	1.59	203.40↓	8.80	6.60	5.68↑
	44.30	46.90	56.52↑	23.31	19.21	6.00↓
	–	–	–	49.12	44.20	7.25↑
7 % wt	−27.50	−37.70	113.90↑	−36.90	−24.13	1.34↑
	−3.02	−3.11	0.35↑	0.26	3.10	66.2↑
	6.90	5.51	2.19↓	6.51	8.93	5.14↓
	18.80	8.10	251.32↓	18.43	23.20	6.55↑
	46.30	52.23	54.33↑	43.90	50.70	7.92↓
	−22.40	−33.40	10.76↑	−36.80	−41.52	3.85↑

Note: The enthalpy values with the arrow pointing up correspond to enthalpy for exothermic behaviors (↑), and the values with arrows pointing down correspond to endothermic enthalpies (↓).

nanotubes. The enthalpy associated with the temperature of −24 ± 4 °C (soft segments) exhibited an increase in the percentage of carbon nanotubes for samples with 1 %, 5 %, and 7 % wt. In contrast, the enthalpy linked to the temperature of 48 °C ± 4 °C (hard segments) remained nearly constant. However, the sample with 3 % wt showed an irregularity, as its enthalpy values at both −24 °C and 48 °C were significantly higher than those presented by the sample with 7 wt % [1–3]. Regarding the enthalpy associated with the melting temperature of the soft segments, around 14 °C, we observed values of 120.96 J/g for TPU-1%, 352.75 J/g for TPU-3%, 417.82 J/g for TPU-5%, and 456.25 J/g for TPU-7%. The noteworthy increase in the enthalpy of fusion can be attributed to the restrictive effect of MWCNTs on the TPU matrix [23]. A comparison between thermoplastic polyurethane incorporated with graphene oxide and thermally reduced graphene oxide suggests that reduction is not always necessary [5,23–26].

Table 2 show the thermal characteristics and enthalpic changes associated with TPU films at different carbon nanotube concentrations, providing valuable information for further research and development in the field of polymer composites. The obtained temperature data revealed distinct melting peaks during the heating cycle for all TPU/MWCNTs film compositions [24,26–29]. As the concentration of MWCNTs increased, the T_{peak} values generally shifted towards higher temperatures, indicating a modified thermal behavior. The T_{Onset} values also showed variations, suggesting changes in the onset of the melting process. The enthalpy changes provided valuable insights into the energy absorbed or released during the phase transitions. For the heating cycle, the enthalpy values

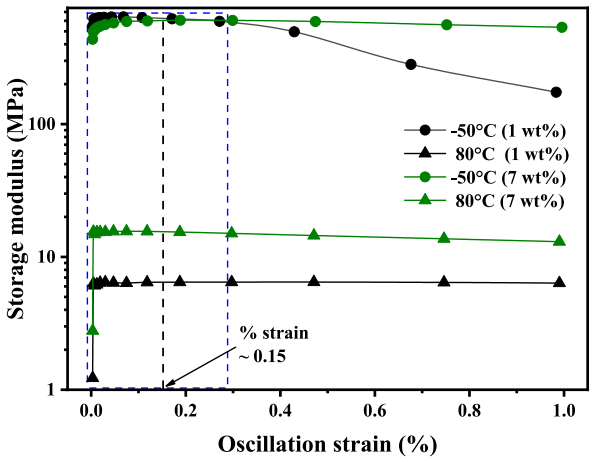

Fig. 3. Storage Modulus versus temperature of TPU/MWCNTs films.

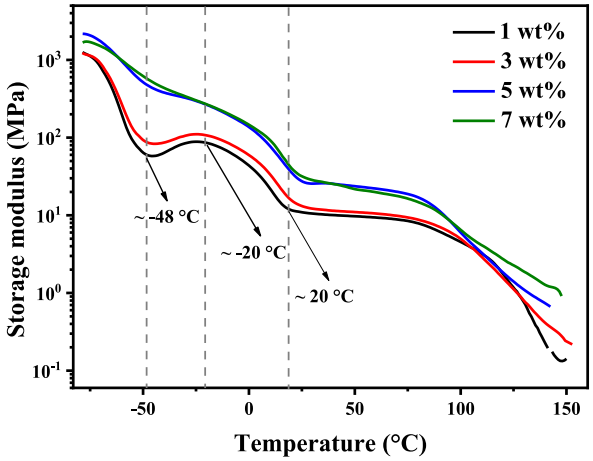

Fig. 4. Storage modulus curves of TPU/MWCNTs.

exhibited both upward and downward trends. The positive enthalpies (↑) indicated exothermic behaviors associated with energy release, while the negative enthalpies (↓) represented endothermic processes with energy absorption. These observations highlight the influence of MWCNTs on the energy storage/release capabilities of the TPU films [30–33].

During the cooling cycle, similar trends were observed in the enthalpy values. The positive enthalpies (↑) indicated exothermic cooling behavior, while the negative enthalpies (↓) indicated endothermic cooling processes. These results further emphasized the impact of MWCNTs on the thermal behavior of the TPU films during cooling.

Enthalpy, a thermodynamic property, is an essential parameter that reveals the energy changes associated with phase transitions or reactions occurring within the TPU/CNT films. In this context, Table 2 provides valuable insights into the enthalpies exhibited by the TPU films at various concentrations of carbon nanotubes. Moreover, the characteristic peaks observed during the heating and cooling cycles allow for the identification of exothermic or endothermic transitions.

3.2. Viscoelastic behavior of TPU/MWCNTs films

3.2.1. Strain sweeps

The behavior of the storage modulus as a function of strain percentage at −50 °C and 80 °C is presented in Fig. 3. The results demonstrate that the values of the storage modulus decrease as temperature increases and increase with the content of MWCNTs. This is due to the softening effect of the TPU matrix at higher temperatures and the stiffening effect of the MWCNTs. A linear viscoelastic region is observed up to 0.2 % strain for all films within the studied temperature range. A strain of 0.15 % was selected for temperature sweeps.

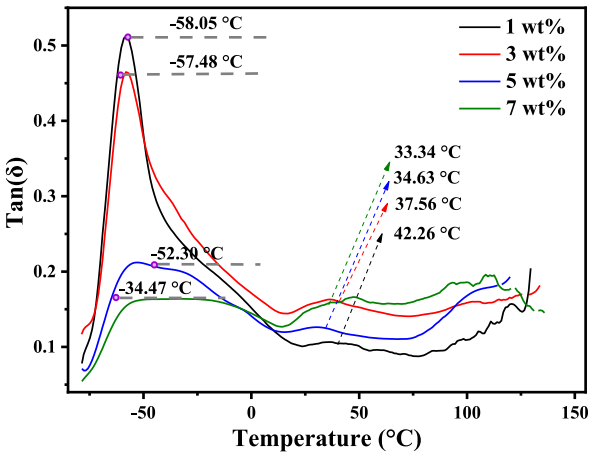

Fig. 5. Tan(delta) curves of TPU/MWCNTs films.

Table 3
Glass transition temperature (T_g) and melting temperature (T_m) of the TPU/MWCNTs films.

TPU/MWCNTs films (wt%)	T_g band		T_m band	
	Temperature range (°C)	Maximum peak T_g (°C)	Temperature range (°C)	Maximum peak T_m (°C)
1.0	−77–23	−58	23–53	42
3.0	−77–15	−57	16–54	37
5.0	−77–14	−52	14–54	34
7.0	−77–14	−34	14–66	33

3.2.2. Temperature sweeps

The curves in Fig. 4 show the elastic responses to deformation called storage modulus as a function of temperature. The storage modulus improves with MWCNTs content for all the films, but the most significant change is seen for the 5 % and 7 % wt. film; This change indicates that the carbon nanofillers have a strong effect on the elastic properties of the TPU matrix due to the restricted movement of the TPU chains. This increase in storage modulus could be attributed to a strong interfacial interaction between the MWCNTs and the TPU matrix [34].

Another crucial aspect to highlight in the observed response is the distinction of four temperature regions. The first region is below −48 °C, followed by the second one between −48 °C and −20 °C. The third region spans from −20 °C to 20 °C, and finally, the fourth region is above 20 °C. Within the first three regions, a notable shift in the storage modulus is observed. In the first and third regions, a strong loss of the storage modulus is observed, associated with the glass transition temperature and the melting temperature mentioned above. However, in the second region, the storage modulus increases, reaching a maximum of about −20 °C. The literature reported that the T_g value for Sui, Guopeng, was around −32 °C. In the case of Ehteramian, Maryam, they found T_g at −23.8 °C [4], and for Rostami, Amir, and Mehdi I. Moosavi they reported it at −27.6 °C [9]. There is a similarity in the literature with region 2, with which it can be assumed that there is a T_g' for the soft segments. But, in the case of the Tan(delta) response, it is overlapped with the band whose maximum intensity is around −57 °C.

Fig. 5 shows Tan(delta) plots with two representative bands, which are reproduced in all the films but with variation in the maximum temperature peak and the average width in each band. The first band observed can be associated with the value of the glass transition temperature of the TPU matrix, and the second band could be associated with the melting temperature of the interaction between the hard and soft segments, T_m(SD/HD), of the TPU matrix previously describe in DSC analysis [4,9,35].

Table 3 shows the temperature ranges and the maximum intensity peak for the bands associated with T_g and T_m. The maximum value associated with the T_g band of the samples 1, 3, 5, and 7 wt% changes to higher temperature values when the percentage of nanotubes increases, this temperature change would indicate that the MWCNTs were adequately dispersed in the TPU matrix, and the TPU/MWCNTs matrix interaction would hinder the movement of the polymeric chains [36].

The decrease in the intensity of the T_g band as the percentage of MWCNTs increases is related to the internal friction between the different elements that make up the system (matrix-matrix, matrix-nanotubes, nanotubes-nanotubes) when the material is subject to external stresses [26,34,37]. In the case of the maximum peak of the T_m band, it moves to lower temperatures with the increase in the concentration of carbon nanotubes in the TPU matrix.

The DSC analysis validates the thermal properties elucidated in Section 3.1 (The thermal properties) by identifying distinctive characteristic peaks and temperature ranges. Notably, the conspicuous exothermic band observed at approximately −20 °C. Additionally, the DSC analysis discerns discrete temperature peaks corresponding to the melting temperature of soft segments (T_m(SS)),

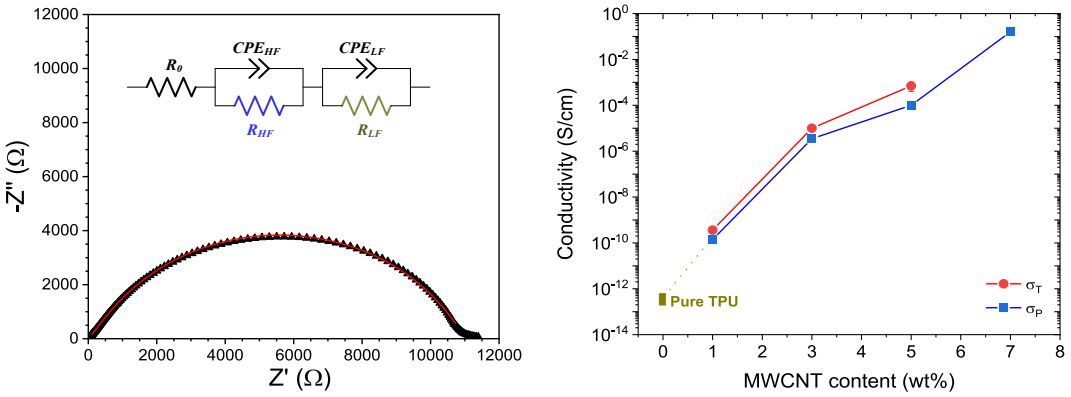

Fig. 6. (left) Complex impedance plot for the TPU films with 3 wt% MWCNTs. (Right) Plot of the electrical conductivity as a function of the MWCNTs content. σ_T and σ_P represent the tunneling and percolation conductivity for each system. The conductivity value for the pure TPU was extracted from [40,44].

interactions between soft and hard segments (T_m(SS/HS)), and the ordering of hard segments (T_m(HS)), all of which were expounded upon in relation to the thermal characteristics of the TPU matrix. Consequently, the comprehensive synthesis of these sections establishes a direct correlation between the described thermal properties and the precise peaks and transitions observed during the DSC analysis. This congruence not only substantiates the initial thermal assertions but also provides further insights into the intricate thermal behavior exhibited by the TPU/MWCNTs films.

3.3. Electrical properties of TPU/MWCNTs films

An electrical characterization of the TPU/MWCNTs nanocomposite films was carried out through impedance spectroscopy (IS) experiments performed at room temperature. Like previous work performed on TPU/MWCNTs nanocomposite plates reported in Ref. [12], conductivity values of different conduction mechanisms have been determined by using an equivalent circuit model on complex impedance plots of -Z''vs Z'. We used the same equivalent circuit that was previously employed to fit the impedance measurements of TPU/MWCNTs plates, and it revealed the presence of percolation and tunneling conduction. Both conduction mechanisms were easily observed in the TPU films with 1, 3 and 5 wt% of MWCNTs (Fig. 6 illustrate one of them). However, it was not possible to observe the electronic tunneling conduction in the film with the maximum MWCNTs concentration studied here (7 wt%); the excellent conductivity of the percolation process for the film (its values exceed those previously reported for TPU/CNT composites with the same weight fraction [12,38–43]) exceeded the sensitivity of the dielectric test fixture to measure small currents.

As it is well-known, the incorporation of carbon nanotubes into the TPU polymer matrix enhances the electronic conductivity of the nanocomposite, reaching a conductivity value of 0.16 S/cm for 7 wt% MWCNTs. It is important to notice that, in comparison to the conductivity tendency observed in the plates, there is not an important increase in conductivity when the TPU is doped with 1 wt% MWCNTs. On the contrary, a progressive increase is observed (on a logarithmic scale), suggesting that a drastic reduction in thickness of the nanocomposite (to the scale hundreds of microns) would facilitate better control of the conductivity properties of carbon nanotube doped TPU systems [45–51].

4. Conclusion

In conclusion, this study investigated the effects of adding MWCNTs to TPU films. The results showed significant improvements in various properties with the inclusion of MWCNTs. The thermal analysis revealed that the incorporation of MWCNTs shifted the T_g to higher temperatures and affected the Tm, indicating changes in the molecular dynamics and crystal behavior of TPU. Through thermal analysis DMA, it was possible to identify that the glass transition temperature of the TPU/MWCNTs mixture ranged from −58 °C to −34 °C, for 1 wt % and 7 wt % of nanotubes respectively. The storage modulus improves in all films, with the most significant change observed between the 1 % and 3 % by weight samples. A similar behavior is observed between the 5 % and 7 % by weight samples, with the enhancement attributed to a strong interfacial interaction between the MWCNTs and the TPU matrix. Impedance spectroscopy studies indicated a substantial increase in the conductivity of the TPU films with the inclusion of MWCNTs. The MWCNTs acted as conductive pathways, improving the electrical properties of the material, and suggesting potential applications in energy storage and electronic devices. In general, the homogeneous dispersion of MWCNTs within the TPU matrix has a positive influence on the thermal, viscoelastic, and electrical properties of TPU films. These results contribute to the development of nanocomposite materials with tailored properties for various applications. Further research is needed to optimize the dispersion of MWCNTs and explore specific industrial applications for TPU/MWCNTs nanocomposites.

CRediT authorship contribution statement

Jose Munoz Chilito: Conceptualization, Formal analysis, Methodology, Writing – original draft. **Jose A. Lara-Ramos:** Formal analysis, Methodology, Writing – original draft. **JulianA. Angel:** Formal analysis, Methodology, Writing – original draft. **Fiderman Machuca-Martínez:** Formal analysis, Methodology, Writing – original draft, Writing – review & editing. **Lorena Marín:** Formal analysis, Writing – original draft. **Luis A. Rodriguez:** Conceptualization, Formal analysis, Methodology, Writing – original draft, Writing – review & editing. **Juan P. Correa Aguirre:** Formal analysis, Methodology, Writing – original draft. **Miguel A. Hidalgo Salazar:** Conceptualization, Formal analysis, Methodology, Supervision, Writing – original draft, Writing – review & editing. **Serafin García-Navarro:** Formal analysis, Methodology, Writing – original draft. **Luis Roca-Blay:** Formal analysis, Methodology, Writing – original draft. **JesusE. Diosa:** Conceptualization, Formal analysis, Methodology, Writing – original draft, Writing – review & editing. **Edgar Mosquera-Vargas:** Conceptualization, Formal analysis, Funding acquisition, Methodology, Project administration, Writing – original draft, Writing – review & editing.

Declaration of competing interest

The authors declare that they have no known competing financial interests or personal relationships that could have appeared to influence the work reported in this paper.

Acknowledgments

We are very grateful to Minciencias (CTeI-SGR BPIN2020000100377). This work is supported by the Universidad del Valle (Strengthening of Centers and Institutes) and the Universidad Autónoma de Occidente.

Appendix A. Supplementary data

Supplementary data to this article can be found online at https://doi.org/10.1016/j.heliyon.2024.e32794.

References

[1] F. Pouladzadeh, A.A. Katbab, N. Haghighipour, E. Kashi, Carbon nanotube loaded electrospun scaffolds based on thermoplastic urethane (TPU) with enhanced proliferation and neural differentiation of rat mesenchymal stem cells: the role of state of electrical conductivity, Eur. Polym. J. 105 (2018) 286–296, https://doi.org/10.1016/j.eurpolymj.2018.05.011.
[2] H. Liu, J. Gao, W. Huang, K. Dai, G. Zheng, C. Liu, C. Shen, X. Yan, J. Guo, Z. Guo, Electrically conductive strain sensing polyurethane nanocomposites with synergistic carbon nanotubes and graphene bifillers, Nanoscale 8 (2016) 12977–12989, https://doi.org/10.1039/C6NR02216B.
[3] Y. Kanbur, U. Tayfun, Investigating mechanical, thermal, and flammability properties of thermoplastic polyurethane/carbon nanotube composites, J. Thermoplast. Compos. Mater. 31 (2018) 1661–1675, https://doi.org/10.1177/0892705717743292.
[4] M. Ehteramian, I. Ghasemi, H. Azizi, M. Karrabi, Functionalization of multi-walled carbon nanotube and its effect on shape memory behavior of nanocomposite based on thermoplastic polyurethane/polyvinyl chloride/multi-walled carbon nanotube (TPU/PVC/MWCNT), Iran. Polym. J. (Engl. Ed.) 30 (2021) 411–422, https://doi.org/10.1007/s13726-021-00900-5.
[5] X.Z. Wang, J.W. Wang, H.Q. Wang, G.C. Zhuang, J.B. Yang, Y.J. Ma, Y. Zhang, H. Ren, Effects of a new compatibilizer on the mechanical properties of TPU/PEBA blends, Eur. Polym. J. 175 (2022) 111358, https://doi.org/10.1016/j.eurpolymj.2022.111358.
[6] A. Laukaitienė, V. Jankauskaitė, K. Žukienė, V. Norvydas, S. Munassipov, U. Janakhmetov, Investigation of polyvinyl chloride and thermoplastic polyurethane waste blend miscibility, Mater. Sci. 19 (2013) 397–402, https://doi.org/10.5755/j01.ms.19.4.3145.
[7] H.M. Jeong, J.H. Song, S.Y. Lee, B.K. Kim, Miscibility and shape memory property of poly(vinyl chloride)/thermoplastic polyurethane blends, J. Mater. Sci. 36 (2001) 5457–5463, https://doi.org/10.1023/A:1012481631570.
[8] S. Kumar, T.K. Gupta, K.M. Varadarajan, Strong, stretchable and ultrasensitive MWCNT/TPU nanocomposites for piezoresistive strain sensing, Compos. B Eng. 177 (2019) 107285, https://doi.org/10.1016/j.compositesb.2019.107285.
[9] A. Rostami, M.I. Moosavi, High-performance thermoplastic polyurethane nanocomposites induced by hybrid application of functionalized graphene and carbon nanotubes, J. Appl. Polym. Sci. 137 (2020) 48520, https://doi.org/10.1002/app.48520.
[10] J. Tang, Y. Wu, S. Ma, T. Yan, Z. Pan, Flexible strain sensor based on CNT/TPU composite nanofiber yarn for smart sports bandage, Compos. B Eng. 232 (2022) 109605, https://doi.org/10.1016/j.compositesb.2021.109605.
[11] P. Russo, M. Lavorgna, F. Piscitelli, D. Acierno, L. Di Maio, Thermoplastic polyurethane films reinforced with carbon nanotubes: the effect of processing on the structure and mechanical properties, Eur. Polym. J. 49 (2013) 379–388, https://doi.org/10.1016/j.eurpolymj.2012.11.008.
[12] J. Muñoz-chilito, J.A. Lara-ramos, L. Mar, F. Machuca-mart, J.P. Correa-aguirre, M.A. Hidalgo-salazar, L. Roca-blay, L.A. Rodr, E. Mosquera-vargas, E. Diosa, Morphological electrical and hardness characterization of carbon nanotube-reinforced thermoplastic polyurethane (TPU) nanocomposite plates, Molecules 28 (2023) 3598, https://doi.org/10.3390/molecules28083598.
[13] S. Kabir, H. Kim, S. Lee, Physical property of 3D-printed sinusoidal pattern using shape memory TPU filament, Textil. Res. J. 90 (2020) 2399–2410, https://doi.org/10.1177/0040517520919750.
[14] M. Asensio, V. Costa, A. Nohales, O. Bianchi, C.M. Gómez, Tunable structure and properties of segmented thermoplastic polyurethanes as a function offlexible segment, Polymers 11 (2019), https://doi.org/10.3390/polym11121910.
[15] S. Valenti, O. Yousefzade, J. Puiggalí, R. Macovez, Phase-selective conductivity enhancement and cooperativity length in PLLA/TPU nanocomposite blends with carboxylated carbon nanotubes, Polymer (Guildf). 191 (2020) 122279, https://doi.org/10.1016/j.polymer.2020.122279.
[16] F. Kucuk, S. Sismanoglu, Y. Kanbur, U. Tayfun, Optimization of mechanical, thermo-mechanical, melt-flow and thermal performance of TPU green composites by diatomaceous earth content, Clean Eng Technol. 4 (2021) 100251, https://doi.org/10.1016/j.clet.2021.100251.
[17] M. Aurilia, F. Piscitelli, L. Sorrentino, M. Lavorgna, S. Iannace, Detailed analysis of dynamic mechanical properties of TPU nanocomposite: the role of the interfaces, Eur. Polym. J. 47 (2011) 925–936, https://doi.org/10.1016/j.eurpolymj.2011.01.005.
[18] S. Kabir, H. Kim, S. Lee, Physical property of 3D-printed sinusoidal pattern using shape memory TPU filament, Textil. Res. J. 90 (2020) 2399–2410, https://doi.org/10.1177/0040517520919750.

[19] X. Suo, Z. Cao, Y. Yu, Y. Liu, Dynamic self-stiffening in polyacrylonitrile/thermoplastic polyurethane composites, Compos. Sci. Technol. 198 (2020) 108256, https://doi.org/10.1016/j.compscitech.2020.108256.

[20] X.Z. Wang, J.W. Wang, H.Q. Wang, G.C. Zhuang, J.B. Yang, Y.J. Ma, Y. Zhang, H. Ren, Effects of a new compatibilizer on the mechanical properties of TPU/PEBA blends, Eur. Polym. J. 175 (2022) 111358, https://doi.org/10.1016/j.eurpolymj.2022.111358.

[21] F. Piana, J. Pionteck, Exploitation of the hard/soft segments ratio in thermoplastic polyurethane (TPU) for the tuning of electrical and mechanical properties of expanded graphite (EG) based composites, SN Appl. Sci. 1 (2019) 1–10, https://doi.org/10.1007/s42452-019-0908-3.

[22] M. Asensio, V. Costa, A. Nohales, O. Bianchi, C.M. Gómez, Tunable structure and properties of segmented thermoplastic polyurethanes as a function offlexible segment, Polymers 11 (2019), https://doi.org/10.3390/polym11121910.

[23] Y. Wang, X. Chen, W. Zhu, X. Huang, X. Tang, J. Yang, A comparison of thermoplastic polyurethane incorporated with graphene oxide and thermally reduced graphene oxide: reduction is not always necessary, J. Appl. Polym. Sci. 136 (2019) 47745, https://doi.org/10.1002/app.47745.

[24] B. Atawa, L. Maneval, P. Alcouffe, G. Sudre, L. David, N. Sintes-Zydowicz, E. Beyou, A. Serghei, In-situ coupled mechanical/electrical investigations on conductive TPU/CB composites: impact of thermo-mechanically induced structural reorganizations of soft and hard TPU domains on the coupled electro-mechanical properties, Polymer (Guildf). 256 (2022), https://doi.org/10.1016/j.polymer.2022.125147.

[25] G. Wang, X. Liao, F. Zou, P. Song, W. Tang, J. Yang, G. Li, Flexible TPU/MWCNTs/BN composites for frequency-selective electromagnetic shielding and enhanced thermal conductivity, Compos. Commun. 28 (2021) 100953, https://doi.org/10.1016/j.coco.2021.100953.

[26] S. Saha, J.P. Singh, U. Saha, T.H. Goswami, K.U.B. Rao, Structure–property relationship of SELF-sustained homogeneous ternary nanocomposites: key issues to evaluate properties of rrP3HT wrapped MWNT dispersed in TPU, Compos. Sci. Technol. 71 (2011) 397–405, https://doi.org/10.1016/j.compscitech.2010.12.005.

[27] X. Luo, H. Cheng, X. Wu, Nanomaterials reinforced polymer filament for fused deposition modeling: a state-of-the-art review, Polymers 15 (2023) 2980, https://doi.org/10.3390/polym15142980.

[28] Y. Wang, W. Li, C. Li, B. Zhou, Y. Zhou, L. Jiang, S. Wen, F. Zhou, Fabrication of ultra-high working range strain sensor using carboxyl CNTs coated electrospun TPU assisted with dopamine, Appl. Surf. Sci. 566 (2021) 150705, https://doi.org/10.1016/j.apsusc.2021.150705.

[29] M. Nofar, B. Batı, E.B. Küçük, A. Jalali, Effect of soft segment molecular weight on the microcellular foaming behavior of TPU using supercritical CO2, J. Supercrit. Fluids 160 (2020), https://doi.org/10.1016/j.supflu.2020.104816.

[30] G.G. Silva, H.D.R. Calado, A.W. Musumeci, W. Martens, E.R. Waclawik, R.L. Frost, G.A. George, Polymer nanocomposites based on P3OT, TPU and SWNT: preparation and characterization. Proceedings of the 2006 International Conference on Nanoscience and Nanotechnology, ICONN, 2006, pp. 182–185, https://doi.org/10.1109/ICONN.2006.340581.

[31] L.B. Gonella, A.J. Zattera, M. Zeni, R.V.B. Oliveira, L.B. Canto, New reclaiming process of thermoset polyurethane foam and blending with polyamide-12 and thermoplastic polyurethane, J. Elastomers Plastics 41 (2009) 303–322, https://doi.org/10.1177/0095244309099413.

[32] M. Nofar, B. Batı, E.B. Küçük, A. Jalali, Effect of soft segment molecular weight on the microcellular foaming behavior of TPU using supercritical CO2, J. Supercrit. Fluids 160 (2020), https://doi.org/10.1016/j.supflu.2020.104816.

[33] S.H. Kang, D.C. Ku, J.H. Lim, Y.K. Yang, N.S. Kwak, T.S. Hwang, Characterization for pyrolysis of thermoplastic polyurethane by thermal analyses, Macromol. Res. 13 (2005) 212–217, https://doi.org/10.1007/BF03219054.

[34] S. Roy, S.K. Srivastava, J. Pionteck, V. Mittal, Montmorillonite-multiwalled carbon nanotube nanoarchitecture reinforced thermoplastic polyurethane, Polym. Compos. 37 (2016) 1775–1785, https://doi.org/10.1002/pc.23350.

[35] G. Sui, D. Liu, Y. Liu, W. Ji, Q. Zhang, Q. Fu, The dispersion of CNT in TPU matrix with different preparation methods: solution mixing vs melt mixing, Polymer (Guildf). 182 (2019) 121838, https://doi.org/10.1016/j.polymer.2019.121838.

[36] X. Suo, Z. Cao, Y. Yu, Y. Liu, Dynamic self-stiffening in polyacrylonitrile/thermoplastic polyurethane composites, Compos. Sci. Technol. 198 (2020) 108256, https://doi.org/10.1016/j.compscitech.2020.108256.

[37] K. Dong, M. Panahi-Sarmad, Z. Cui, X. Huang, X. Xiao, Electro-induced shape memory effect of 4D printed auxetic composite using PLA/TPU/CNT filament embedded synergistically with continuous carbon fiber: a theoretical & experimental analysis, Compos. B Eng. 220 (2021) 108994, https://doi.org/10.1016/j.compositesb.2021.108994.

[38] D. Feng, D. Xu, Q. Wang, P. Liu, Highly stretchable electromagnetic interference (EMI) shielding segregated polyurethane/carbon nanotube composites fabricated by microwave selective sintering, J Mater Chem C Mater 7 (2019) 7938–7946, https://doi.org/10.1039/C9TC02311A.

[39] T.K. Gupta, B.P. Singh, S. Teotia, V. Katyal, S.R. Dhakate, R.B. Mathur, Designing of multiwalled carbon nanotubes reinforced polyurethane composites as electromagnetic interference shielding materials, J. Polym. Res. 20 (2013) 169, https://doi.org/10.1007/s10965-013-0169-6.

[40] Y. Zheng, Y. Li, K. Dai, M. Liu, K. Zhou, G. Zheng, C. Liu, C. Shen, Conductive thermoplastic polyurethane composites with tunable piezoresistivity by modulating the filler dimensionality for flexible strain sensors, Compos Part A Appl Sci Manuf. 101 (2017) 41–49, https://doi.org/10.1016/j.compositesa.2017.06.003.

[41] Y.-S. Jun, B.G. Hyun, M. Hamidinejad, S. Habibpour, A. Yu, C.B. Park, Maintaining electrical conductivity of microcellular MWCNT/TPU composites after deformation, Compos. B Eng. 223 (2021) 109113, https://doi.org/10.1016/j.compositesb.2021.109113.

[42] N.P. Kim, 3D-Printed conductive carbon-infused thermoplastic polyurethane, Polymers 12 (2020) 1224, https://doi.org/10.3390/polym12061224.

[43] A.S. Hoang, Electrical conductivity and electromagnetic interference shielding characteristics of multiwalled carbon nanotube filled polyurethane composite films, Adv. Nat. Sci. Nanosci. Nanotechnol. 2 (2011) 025007, https://doi.org/10.1088/2043-6262/2/2/025007.

[44] H. Liu, J. Gao, W. Huang, K. Dai, G. Zheng, C. Liu, C. Shen, X. Yan, J. Guo, Z. Guo, Electrically conductive strain sensing polyurethane nanocomposites with synergistic carbon nanotubes and graphene bifillers, Nanoscale 8 (2016) 12977–12989, https://doi.org/10.1039/C6NR02216B.

[45] R.I. Revilla, B. Wouters, F. Andreatta, A. Lanzutti, L. Fedrizzi, I. De Graeve, EIS comparative study and critical Equivalent Electrical Circuit (EEC) analysis of the native oxide layer of additive manufactured and wrought 316L stainless steel, Corros Sci 167 (2020) 108480, https://doi.org/10.1016/j.corsci.2020.108480.

[46] F. Stan, R.T. Rosculet, C. Fetecau, Direct Current method with reversal polarity for electrical conductivity measurement of TPU/MWCNT composites, Measurement 136 (2019) 345–355, https://doi.org/10.1016/j.measurement.2018.12.107.

[47] S. Kumar, T.K. Gupta, K.M. Varadarajan, Strong, stretchable and ultrasensitive MWCNT/TPU nanocomposites for piezoresistive strain sensing, Compos. B Eng. 177 (2019) 107285, https://doi.org/10.1016/j.compositesb.2019.107285.

[48] D.A. Harrington, P. van den Driessche, Mechanism and equivalent circuits in electrochemical impedance spectroscopy, Electrochim. Acta 56 (2011) 8005–8013, https://doi.org/10.1016/j.electacta.2011.01.067.

[49] G. Wu, Z. Yang, Z. Zhang, B. Ji, C. Hou, Y. Li, W. Jia, Q. Zhang, H. Wang, High performance stretchable fibrous supercapacitors and flexible strain sensors based on CNTs/MXene-TPU hybrid fibers, Electrochim. Acta 395 (2021) 139141, https://doi.org/10.1016/j.electacta.2021.139141.

[50] S.J. Kwon, S.H. Ryu, Y.K. Han, J. Lee, T. Kim, S.-B. Lee, B. Park, Electromagnetic interference shielding films with enhanced absorption using double percolation of poly (methyl methacrylate) beads and CIP/MWCNT/TPU composite channel, Mater. Today Commun. (2022) 103401, https://doi.org/10.1016/j.mtcomm.2022.103401.

[51] B.-A. Mei, O. Munteshari, J. Lau, B. Dunn, L. Pilon, Physical interpretations of nyquist plots for EDLC electrodes and devices, J. Phys. Chem. C 122 (2018) 194–206, https://doi.org/10.1021/acs.jpcc.7b10582.